This is an open access article published under a Creative Commons Non-Commercial No Derivative Works (CC-BY-NC-ND) Attribution License, which permits copying and redistribution of the article, and creation of adaptations, all for non-commercial purposes.

ACS AUTHORCHOICE

ACS chemical biology

pubs.acs.org/acschemicalbiology

Articles

C-Mannosyl Lysine for Solid Phase Assembly of Mannosylated Peptide Conjugate Cancer Vaccines

Tim P. Hogervorst,[§] R. J. Eveline Li,[§] Laura Marino, Sven C. M. Bruijns, Nico J. Meeuwenoord, Dmitri V. Filippov, Herman S. Overkleeft, Gijsbert A. van der Marel, Sandra J. van Vliet, Yvette van Kooyk,* and Jeroen D. C. Codée*

Cite This: https://dx.doi.org/10.1021/acschembio.9b00987

Read Online

ACCESS | Metrics & More | Article Recommendations | Supporting Information

ABSTRACT: Dendritic cells (DCs) are armed with a multitude of Pattern Recognition Receptors (PRRs) to recognize pathogens and initiate pathogen-tailored T cell responses. In these responses, the maturation of DCs is key, as well as the production of cytokines that help to accomplish T cell responses. DC-SIGN is a frequently exploited PRR that can effectively be targeted with mannosylated antigens to enhance the induction of antigen-specific T cells. The natural *O*-mannosidic linkage is susceptible to enzymatic degradation, and its chemical sensitivity complicates the synthesis of mannosylated antigens. For this reason, (oligo)mannosides are generally introduced in a late stage of the antigen synthesis, requiring orthogonal conjugation handles for their attachment. To increase the stability of the mannosides and streamline the synthesis of mannosylated peptide antigens, we here describe the development of an acid-stable *C*-mannosyl lysine, which allows for the inline introduction of mannosides during solid-phase peptide synthesis (SPPS). The developed amino acid has been successfully used for the assembly of both small ligands and peptide antigen conjugates comprising an epitope of the gp100 melanoma-associated antigen and a TLR7 agonist for DC activation. The ligands showed similar internalization capacities and binding affinities as the *O*-mannosyl analogs. Moreover, the antigen conjugates were capable of inducing maturation, stimulating the secretion of pro-inflammatory cytokines, and providing enhanced gp100 presentation to $CD8^+$ and $CD4^+$ T cells, similar to their *O*-mannosyl counterparts. Our results demonstrate that the *C*-mannose lysine is a valuable building block for the generation of anticancer peptide-conjugate vaccine modalities.

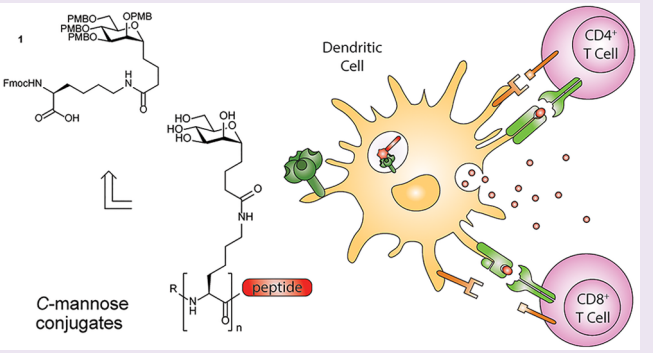

Downloaded via LEIDEN UNIV on March 6, 2020 at 14:17:38 (UTC).
See https://pubs.acs.org/sharingguidelines for options on how to legitimately share published articles.

Immunotherapy for cancer is gaining momentum. More and more therapies have reached the clinic or are in advanced clinical trials, including immune checkpoint blocking (ICB) antibodies, chimeric antigen receptor T cells (CAR T cells), adoptive cell transfer (ACT), and dendritic cell (DC) vaccination.[1−4] DC-based strategies rely on the role of dendritic cells as key initiators of the adaptive immune system that are crucial in the induction of memory responses. Via antigen capture and processing, DCs can present peptides to naïve T lymphocytes and skew their differentiation end points, and by exposing DCs to synthetic tumor (neo-)antigens, the immune response can be directed toward specific cancer-associated antigens. Although animal models have demonstrated promising results for peptide-based vaccine strategies, human trials often result in minimal tumor regression and only partial effectiveness.[5,6] Vaccine efficacy may be improved by the incorporation of adjuvants that can target Pattern Recognition Receptors (PRRs), which can induce DC maturation and improve antigen processing.[7] Toll-Like Receptors (TLRs) are a family of PRRs, of which members have been successfully targeted with covalent adjuvant-antigen conjugates,[8−12] to induce DC maturation and improve antigen processing and presentation.[13,14] Another family of PRRs that has frequently been exploited as an endocytic receptor to facilitate antigen cross-presentation is the C-type Lectin Receptors (CLRs). This family of PRRs recognizes carbohydrate patterns and is an essential determinant in discerning host from foreign antigens. An often studied receptor is DC-SIGN (CD209), a CLR present on DCs that internalizes carbohydrate modified antigens for cross-presentation to T cells. DC-SIGN recognizes mannose and Lewis-type carbohydrate moieties on a wide variety of pathogens and is often targeted to activate specific signaling and tailor the immune response.[15] DC-SIGN can also act as a scavenger receptor that

Received: December 9, 2019
Accepted: February 11, 2020
Published: February 11, 2020

© XXXX American Chemical Society

Scheme 1. Synthesis of *C*-Mannoside Lysine 1[a]

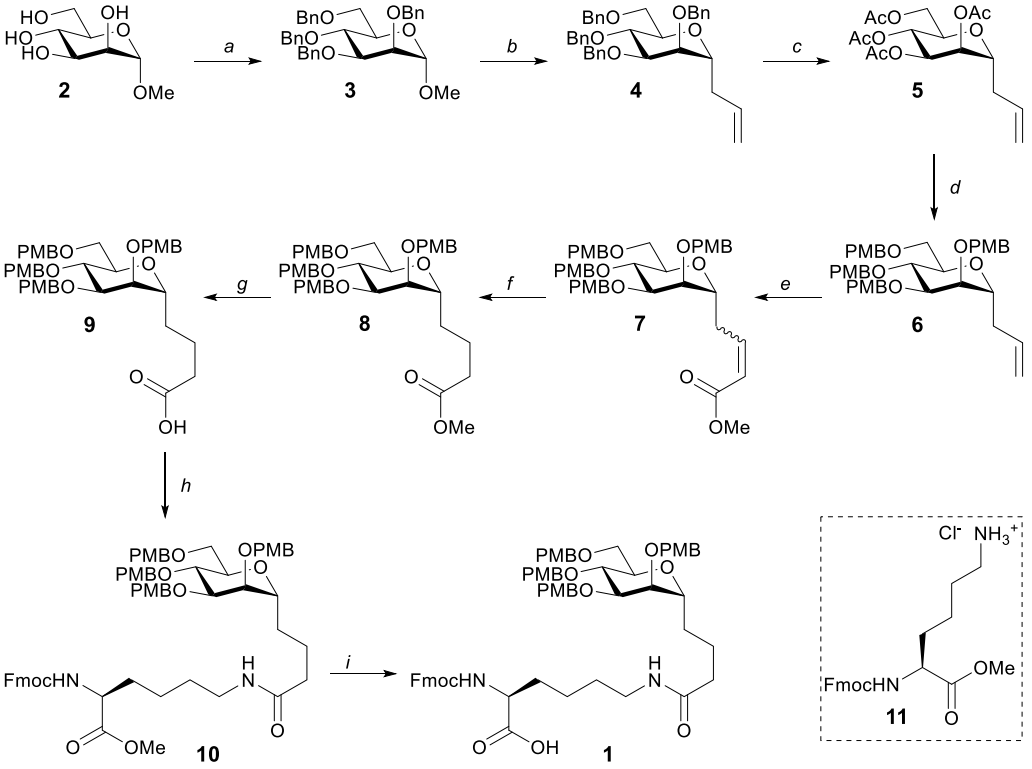

[a]Reagents and conditions: (a) NaH, BnBr, TBAI, DMF, 78%; (b) allylTMS, TMSOTf, ACN, 73%; (c) either (*i*) BCl_3, DCM and (*ii*) Ac_2O, pyridine 95% or (*i*) Li, naphthalene, THF, −20 °C and (*ii*) Ac_2O, pyridine, 54%; (d, *i*) NaOMe, MeOH, (*ii*) NaH, PMBCl, TBAI, DMF, 69%; (e) methyl acrylate, Grubbs second gen. catalyst, DCM, 73%; (f) $RuCl_3$, $NaBH_4$, DCE/MeOH, 93%; (g) KOH, THF/H_2O, qnt.; (h) **11**, HCTU, DIPEA, DMF, 99%; (i) LiOH, H_2O_2, THF/H_2O/*t*-BuOH, 79%.

can induce receptor-mediated endocytosis. Due to its tetramic structure, a multivalent presentation of its ligand enhances the avidity for DC-SIGN. Thus, while the affinity for a single monomannoside ligand is low, targeting mannosylated constructs can be markedly increased by the multivalent presentation of the monosaccharides on a polyvalent core or carrier platform such as dendrimers, liposomes, or nanoparticles.[16−18] Vaccination with mannosylated antigens in mice has demonstrated improved cytotoxic lymphocyte responses, stronger Th1 and Th2 responses, and increased antibody responses.[19] The addition of an adjuvant can further boost the generated immune response of mannosylated conjugates. For example, the conjugation of multivalent mannosides and TLR7 adjuvants to an antigen via a self-immolative linker resulted in a more robust and higher-quality humoral and cellular immune response in mice.[20]

In earlier work, we have also demonstrated the significance of antigen mannosylation.[21] We systematically increased the number of well-defined mono-, di-, and trimannosides on a peptide backbone to evaluate the effect of multivalent presentation of DC-SIGN ligands on the peptide antigens. We could also extend the conjugates with a secondary adjuvant. Using this strategy, we generated precisely defined trifunctional conjugates (CLR-antigen-TLR), which effectively targeted DC-SIGN.[21] This approach, however, required the conjugation of *O*-mannosides via a Cu(I) catalyzed azide−alkyne cycloaddition (CuAAC), which involved an additional purification step and limits the number of available orthogonal handles that can be incorporated into the conjugates. Furthermore, *O*-mannosides may be enzymatically cleaved, rendering them less suitable for DC-SIGN targeting.[16,22,23] Therefore, we here report the design and synthesis of a *C*-mannose functionalized lysine building block (**1**, Scheme 1). This *C*-mannoside lacks the exocyclic anomeric oxygen to render the glycosidic linkage resistant to the acidic conditions necessary for standard automated solid phase peptide synthesis (SPPS). In addition, the *C*-glycoside is resistant to enzymatic hydrolysis. By attachment to an Fmoc-protected amino acid building block, the mannoside can be incorporated via "inline" synthetic methodology, obviating postsynthesis conjugation steps and preventing the use of an azide−alkyne click reaction. The *C*-mannoside building block has been used to generate peptide-antigen conjugates, carrying one or six mannosides, in addition to a synthetic TLR7 ligand. The generated constructs have been evaluated, in a side by side comparison to the corresponding *O*-mannoside clusters, for binding affinity, uptake, and antigen presentation capacity, revealing that *C*-mannosides can effectively be used to replace their more labile *O* counterparts in covalent antigen conjugates.

RESULTS AND DISCUSSION

Synthesis of the *C*-Mannoside Lysine Building Block.

The synthesis of the key SPPS-ready mannosylated Fmoc amino acid is achieved in 11 steps and is shown in Scheme 1. The crucial step in the synthesis of **1** is the introduction of the α-*C*-glycosidic bond. On the basis of previously reported work by Girard et al.,[24] the anomeric allyl was introduced via a Hosomi−Sakurai reaction using allyltrimethylsilane (allyl-TMS). The synthesis starts from methyl 2,3,4,6-tetra-*O*-benzyl-α-D-mannopyranoside **3**, obtained by benzylation of

https://dx.doi.org/10.1021/acschembio.9b00987
ACS Chem. Biol. XXXX, XXX, XXX−XXX

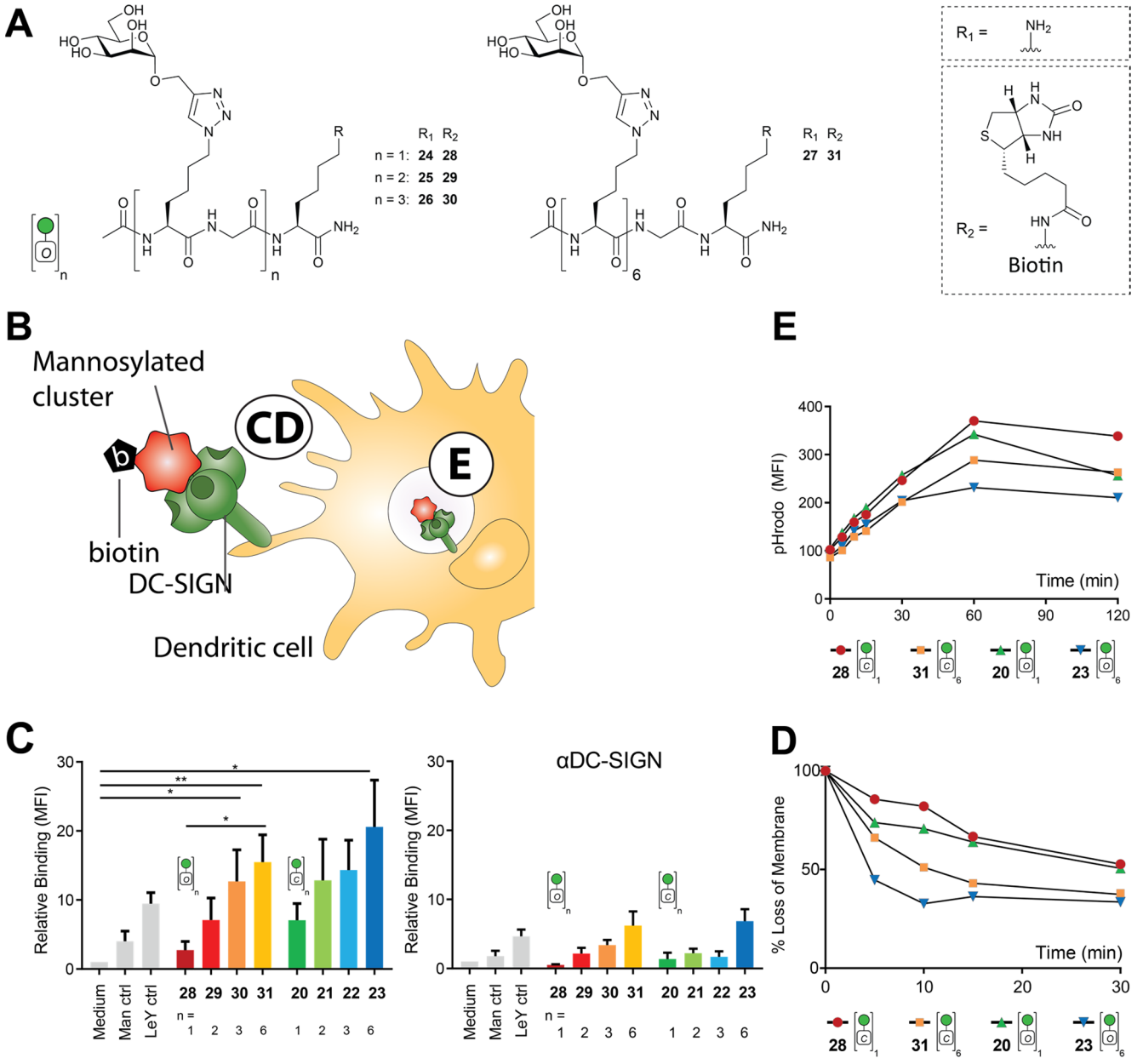

Figure 1. Binding of the *C*-mannoside clusters to DC-SIGN. (A) Structure of the mono-, di-, tri-, or hexavalent *O*-mannoside clusters, with and without biotin. (B) Schematic representation of the binding, internalization, and endosomal routing assays. (C) Binding of the biotinylated clusters to moDC DC-SIGN as measured by flow cytometry (left panel, eight donors) and to moDC with blocked DC-SIGN (right panel). Polyacrylamide decorated with monomannosides or Le^Y antigens were used as positive controls. Paired Student's *t* test error: $*p < 0.05$; $**p < 0.001$. (D) DC-SIGN-mediated internalization of the clusters was measured by flow cytometry. One donor is depicted as a representative of four individuals. (E) The routing of the clusters to the endosomes/lysosomes as measured by flow cytometry and normalized to a negative control. One donor is depicted as representative of three individuals.

methyl α-D-mannopyranoside **2**. [The use of per-acetylated mannosyl donors has previously been shown to lead to anomeric mixtures, indicating that neighboring group participation falls short in effecting stereoselective *C*-glycosylation reactions.[21−25]] The allyl group was introduced by treatment of the methyl mannoside with allyltrimethyl silane and trimethylsilyl triflate in acetonitrile to provide *C*-mannoside **4**. This reaction proceeded with high stereoselectivity and was complete within an hour when assisted by ultrasound irradiation.[25] Selective removal of the benzyl ethers in the presence of the allyl functionality was initially effected using either BCl_3 or a Birch reduction in liquid ammonia.[26] However, both reactions proved difficult to scale up, and we therefore switched to the use of a single electron reduction using lithium naphthalenide in THF. This reaction could be run at 80 mmol scale, to provide the desired tetra-ol, which was acetylated to ease purification, delivering **5** in 54% yield. After the installation of four PMB ethers, the anomeric allyl appendage was elongated through a cross-metathesis with methyl acrylate to afford α,β-unsaturated ester **7**. The reduction of the double bond in this product with $RuCl_3$ in the presence of $NaBH_4$ and MeOH[27] was followed by saponification of the resulting ester **8** to obtain carboxylic acid **9**. Fully protected *C*-mannosyl lysine **12** was obtained by

https://dx.doi.org/10.1021/acschembio.9b00987
ACS Chem. Biol. XXXX, XXX, XXX−XXX

Scheme 2. Synthesis of *C*-Mannoside Clusters[a]

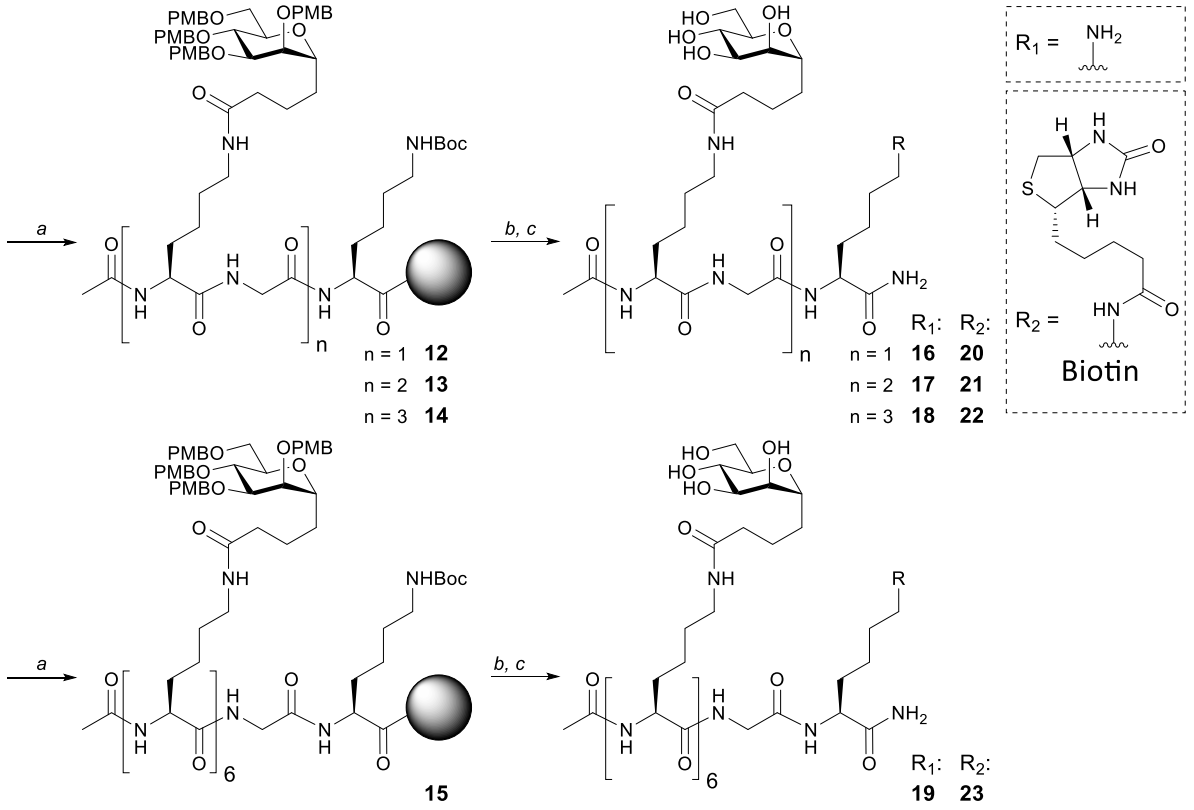

[a]Reagents and conditions: (a) Fmoc-SPPS (**1**, HCTU, DIPEA, DMF); (b) TFA, TIS, H_2O, (octanethiol, phenol; **16**, 7.0%; **17**, 14%; **18**, 6.0%; **19**, 2.1%); (c) BiotinOSu, DIPEA, DMSO (**20**, 94%; **21**, 72%; **22**, 99%; **23**, 80%).

coupling of carboxylic acid **9** with the methyl ester of N_α-Fmoc protected lysine **11**, using HCTU as condensation agent. Selective hydrolysis of the ester in the presence of the Fmoc group was achieved with LiOOH,[28,29] which is more nucleophilic but less basic than LiOH,[30] resulting in the isolation of key building block **1** in 79% yield. Altogether, SPPS-compatible *C*-mannosyl **1** was synthesized in 20% yield over 11 steps.

Synthesis of the Mannoside Clusters. Our previous work has described the synthesis of the *O*-mannoside clusters[21] and resulted in monovalent- (**24**), bivalent- (**25**), trivalent- (**26**), and hexavalent (**27**) O-mannoside clusters. Biotinylation of these compounds resulted in biotinylated O-mannoside clusters **28**, **29**, **30**, and **31**, respectively (Figure 1A). To enable a direct comparison to these clusters, we here generated clusters containing one, two, three, or six copies of the *C*-mannosyl through an SPPS approach (Scheme 2). Using Tentagel S RAM amide resin, Fmoc-Lys(Boc)-OH and Fmoc-Gly-OH were introduced successively, followed by elongation with *C*-mannosyl **1** using a standard Fmoc protocol and HCTU as the condensation agent. Building block **1** was introduced manually, using only a small excess of the amino acid and prolonged coupling times (2 equiv, overnight) to prevent the use of a large excess of **1**. After completion of the sequence, the N-termini were capped with acetyl groups, resulting in immobilized peptides **12**−**15**. Subjecting resins **12**−**15** to a cleavage cocktail of TFA/TIS/H_2O (190/5/5, v/v/v) successfully removed the Boc and PMB ethers, and the peptide clusters were isolated after RP-HPLC purification to obtain monovalent (**16**), bivalent (**17**), trivalent (**18**), and hexavalent (**19**) clusters in 7%, 14%, 6%, and 2% yield, respectively (Scheme 2, R = R_1). Further functionalization via the introduction of a biotin handle was achieved by reacting the primary amine of the C-terminal lysine with a biotin-*N*-hydroxysuccinimide (NHS) ester. This resulted in biotinylated mannoside clusters **20**−**23** (Scheme 2, R = R_2).

Binding of the *C*-Mannoside Clusters to moDCs. With the biotinylated constructs in hand, the effect of the *O* to CH_2 modification was evaluated by studying the binding, internalization, and endosomal routing upon DC-SIGN engagement of the *C*-mannoside clusters and their *O*-mannoside equivalents **28**−**31** (Figure 1A,B).[21] The binding of the clusters to cellular membrane DC-SIGN was evaluated using DC-SIGN expressing monocyte-derived DCs (moDCs; Figure 1C, also see Supporting Information, Figure SI.1A). The assay was performed at a temperature of 4 °C to prevent the internalization of DC-SIGN from the cell membrane surface. The cells were incubated with the biotinylated clusters for 30 min, after which unbound clusters were washed away. Treatment of the cells with fluorophore-labeled streptavidin allowed quantification of binding by flow cytometry. An increase in binding of bivalent *C*-mannoside **21**, trivalent *O*-mannoside **30** and *C*-mannoside **22**, and hexavalent *O*-mannoside **31** and *C*-mannoside **23** was seen when compared to the unstimulated control. Compared to a mannosylated polyacrylamide control, all compounds showed better binding, with the exception of mono-*O*-mannoside **28**. A clear valency-dependent increase in binding was seen within each of the *O*- and *C*-mannoside sets. These results are in line with our previous study, in which we compared the monomannoside

https://dx.doi.org/10.1021/acschembio.9b00987
ACS Chem. Biol. XXXX, XXX, XXX−XXX

Scheme 3. Synthesis of C- and O-Mannoside−gp100−TLR7 Agonist Conjugates[a]

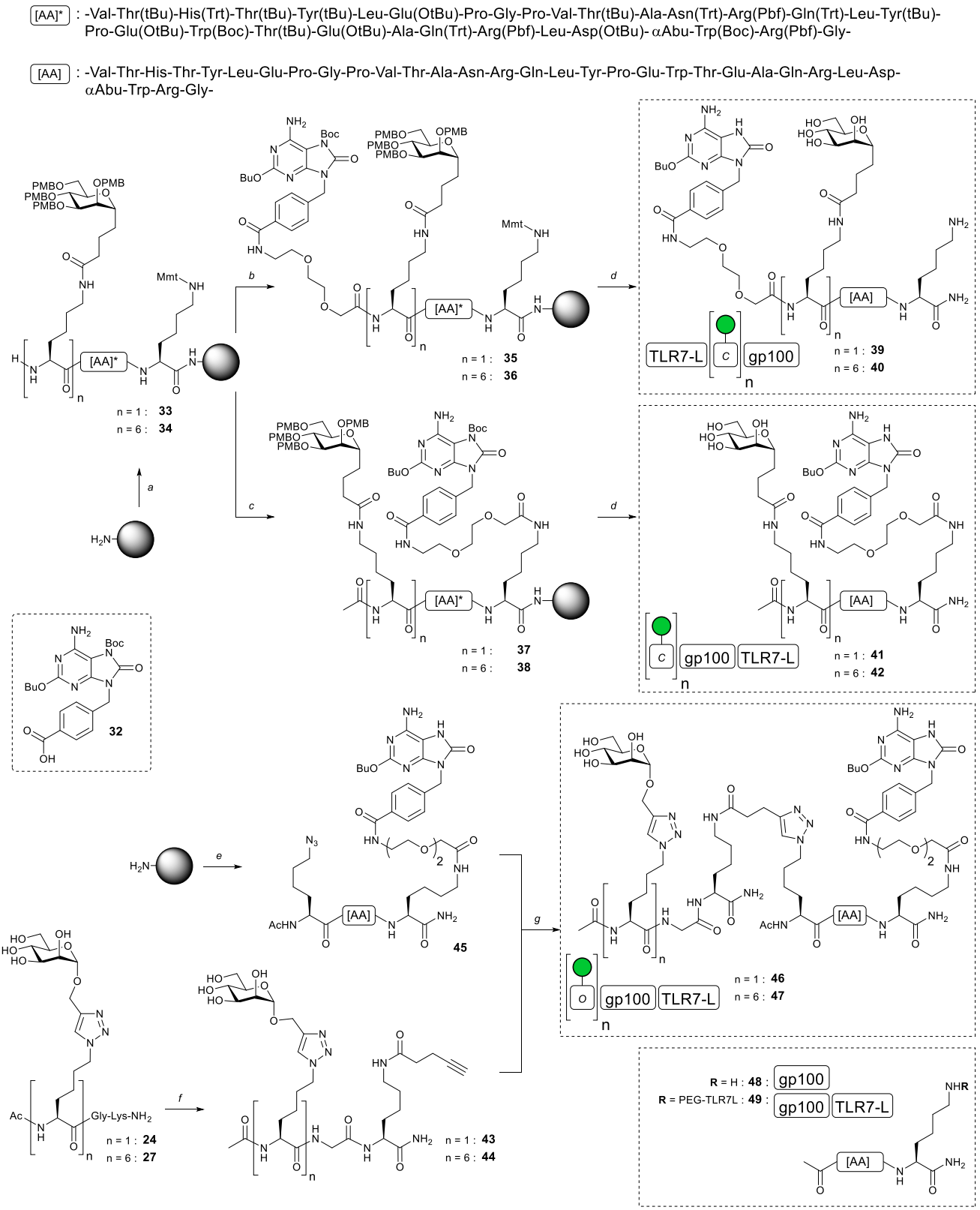

[a]Reagents and conditions: (a) Fmoc-SPPS (**1**, HCTU, DIPEA, DMF); (b) Fmoc-SPPS (Fmoc-AEEA-OH or **32**, HCTU, DIPEA, DMF); (c, *i*) Ac_2O, DIPEA, DMF; (*ii*) AcOH, TFE, DCM; (*iii*) Fmoc-SPPS (Fmoc-AEEA-OH or **32**, HCTU, DIPEA, DMF); (d) TFA, TIS, H_2O, octanethiol, phenol (**39**, 2.60% over 36 couplings; **40**, 1.30% over 41 couplings; **41**, 2.10% over 36 couplings; **42**, 0.60% over 41 couplings); (e) Fmoc-SPPS, see ref 21; (f) pent-4-ynoic acid succinimidyl ester, DIPEA, DMSO (**43**, 62%; **44**, 66%); (g) CuI, THPTA, DIPEA, H_2O, DMSO (**46**, 34%; **47**, 29%).

https://dx.doi.org/10.1021/acschembio.9b00987
ACS Chem. Biol. XXXX, XXX, XXX−XXX

clusters to clusters built up from more complex di- and trimannosides.[21] For all clusters, higher valency led to higher binding affininty. Binding of the hexavalent monomannoside cluster was comparable to the binding of the higher valent di- and trimannosides. Blocking of the DC-SIGN receptor effectively diminished the binding, although low residual binding with a similar valency-dependent increase remained (see SI, Figure SI.1B). The residual binding suggests cluster recognition of other mannose-binding receptors on DCs, such as the mannose receptor.[31]

We next selected the mono- and hexavalent *O*- and *C*-mannoside clusters to assess their internalization. The assessment of cluster internalization was executed at 4 °C, similar to the binding assay. To this end, the cells were incubated for 60 min to saturate the immobilized DC-SIGN receptors at the cell surface, followed by the removal of unbound clusters. Resuspension of the samples in warm (37 °C) medium initiated internalization. At the indicated time points, samples were taken and immediately put on ice. The signal loss of the membrane was measured through flow cytometry upon treatment with a fluorophore-conjugated streptavidin. To exclude cluster-DC-SIGN dissociation, we additionally gently fixed the cells with 1% paraformaldehyde for permanent immobilization of DC-SIGN at the membrane. No dissociation of the mannosylated clusters from DC-SIGN on fixed cells was measured (see SI, Figure SI.1C), indicating that the ligands are internalized upon DC-SIGN binding. Internalization (>50%) of the hexavalent cluster **23** was seen after 5 min (Figure 1D). The complementary *O*-mannoside cluster (**31**) accomplished the same level of internalization after 15 min. Uptake of the monovalent clusters occurred at a slower rate, requiring 30 min for internalization of approximately 50% of both the *O*- and *C*-mannose clusters (**28**, **20**). The relative internalization efficiency seems to mirror the binding profiles seen in Figure 1C.

Mono- and hexavalent cluster trafficking to the endosomes was further studied using pHrodo Red. This dye acts as a pH-sensitive sensor, as the fluorescence is considerably increased in acidic environments, while it is quenched in the neutral extracellular environment. Prior to moDC stimulation, the biotinylated mannoside clusters were treated with the avidin-conjugated fluorophore (2:1). The precomplexed clusters were subsequently added to the moDCs at 37 °C, continued by sample collection at each time point. The cells were washed and gently fixed, and fluorescence was subsequently measured by flow cytometry. After 30 min, a 2-fold increase was visible in the fluorescence of the hexavalent *O*- and *C*-mannoside clusters (Figure 1E). On the other hand, the fluorescence of both monovalent clusters (**28** and **20**) was increased 2.5-fold at 30 min, suggesting higher endosomal ligand concentrations. Although the *C*-mannosides resembled the *O*-mannoside clusters, the deviation between mono- and hexavalent presentation is surprising. In the previous binding and internalization assays, the hexavalent clusters **31** and **23** were superior to monovalent mannoside presentation. The increased MFI of the monovalent over the hexavalent clusters at 30 min could indicate faster endolysosomal trafficking of the smaller clusters, as the emitted fluorescence by the dye is higher with lower pH.[32,33] Moreover, the mannosylated clusters were precomplexed with the pHrodo dye into a larger particle, possibly contributing to the altered endocytosis.[34] Altogether these results indicate that the *C*-mannoside clusters **20** and **23** were able to convincingly resemble the DC-SIGN binding[16] and internalization profiles of the *O*-mannoside equivalents, encouraging the implementation of *C*-mannosylated antigen conjugates.

Synthesis of Mannosylated gp100 Conjugates. Melanoma derived from transformed pigment-carrying melanocytes is a highly lethal cancer, and this malignancy is considered one of the most immunogenic cancer types.[35] We therefore selected the melanoma-associated antigen gp100 as our vaccine target, and we introduced C-terminal mannoside clusters and a secondary TLR ligand to generate self-adjuvating peptide antigen vaccine conjugates.[36] Endosomal TLR7 was selected as a PRR target because we reasoned that the use of a cell surface PRR targeting PAMP would lead to competition for binding with DC-SIGN on the outside of the DC surface membrane. Furthermore, DC-SIGN-mediated endocytosis should deliver the conjugates to the endosomes, where it will encounter the TLR7 receptor. The target gp100 peptide antigen combines the $CD4^+$ T cell binding epitope $gp100_{280-288}$ and $CD8^+$ T cell binding epitope $gp100_{44-59}$. Multiple conjugates were synthesized bearing the TLR7 agonist either on the N or C terminus and carrying either one or six mannosides, to study the effect of these modifications on antigen presentation.

The SPPS of the conjugates started with the introduction of a monomethoxytrityl (Mmt) functionalized Fmoc-Lys-OH on Tentagel S RAM amide resin (Scheme 3). Both termini of the antigen sequence were extended with four naturally occurring amino acids to act as spacers between the antigens, the mannoside cluster, and the TLR7 ligand. The Cys_{60} in the N-terminal spacer was replaced with an isosteric α-amino-butyric acid analog to prevent potential oxidation and peptide dimerization,[37] a modification we previously demonstrated not to affect antigen biology.[21] The sequences were elongated at the *N*-terminus with either one or six copies of the *C*-mannosyl **1**, resulting in immobilized peptides **33** and **34** (Scheme 3). Next, **33** and **34** were further extended at their *N*-termini with the TLR7 ligand 2-butoxy-8-oxo-adenine, using the previously described Boc protected building block **32**,[38] to give immobilized conjugates **35** and **36**. Alternatively, the *N*-termini were acetylated, after which the *C*-termini were further functionalized by selective removal of the *C*-terminal lysine Mmt-group, followed by the introduction of the TLR7 ligand to provide **37** and **38**.[39] It was observed that a cocktail of TFA (1%) in DCM, led to partial removal of the PMB groups leading to the undesired esterification of some of the carbohydrate alcohols with the TLR7 ligand. Therefore, milder conditions were explored for the removal of the *C*-terminal Mmt group. Eventually, the use of acetic acid in a mixture of trifluoroethanol (TFE) and DCM (1/2/7, v/v/v), a cocktail first described to selectively cleave the Mmt over methyltrityl and trityl groups selectively,[40] was found to be effective for the selective unmasking of the MMT in the resin-bound protected conjugates. Using these conditions, the immobilized N-terminal elongated conjugates **37** and **38** were successfully generated.

Initial attempts to deprotect and release the peptides from the resin with a cleavage cocktail of TFA/TIS/H_2O (190/5/5, v/v/v) resulted in complex crude mixtures. Analysis of the mixtures indicated that the poor quality of the crude material was due to side reactions of the cleavage and deprotection step and not due to incomplete couplings. Reactive cationic species are liberated during the acidic removal of the PMB ethers, which can react with functional groups in the unprotected

https://dx.doi.org/10.1021/acschembio.9b00987
ACS Chem. Biol. XXXX, XXX, XXX−XXX

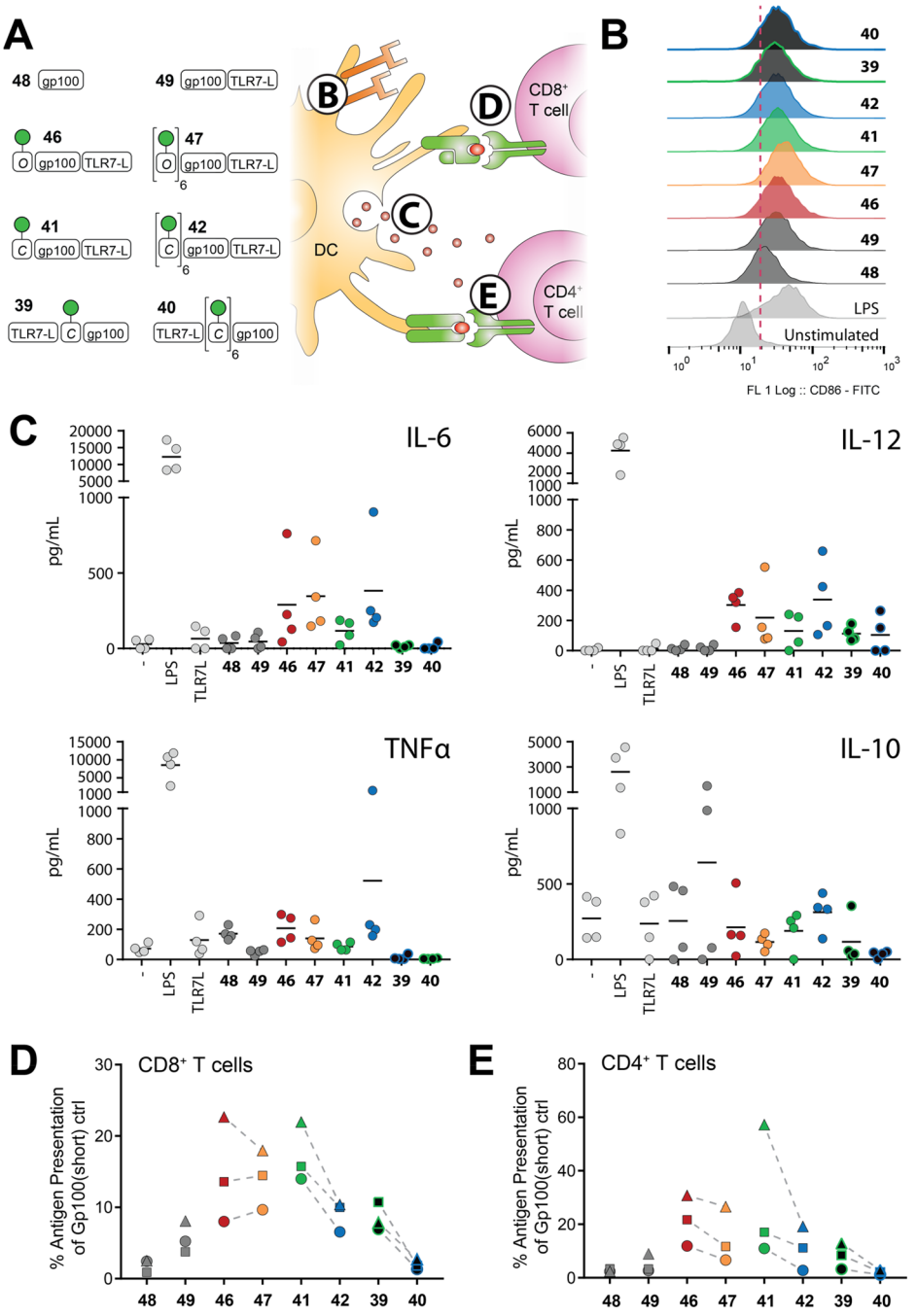

Figure 2. Targeting efficacy of the mannoside-peptide conjugates. (A) Schematic representation of the compounds and overview of the moDC maturation, cytokine secretion, $CD4^+$ and $CD8^+$ T lymphocyte antigen presentation. (B) Expression of costimulatory marker CD86 as measured by flow cytometry. One out of four donors is depicted. LPS and **49** were included as positive controls, as well as **48** as a negative control. (C) IL-6, IL-10, IL-12p70, and TNFα secretion of four donors was measured using ELISA upon overnight stimulation with *O*- or *C*-mannoside conjugates. (D) Antigen presentation capacity of moDCs to $CD8^+$ T lymphocytes was quantified by the IFNγ production of activated T cells. The dashed lines represent the directionality between the donors when comparing mono- and hexavalent mannosides analogs. (E) Antigen presentation capacity of moDCs to $CD4^+$ T lymphocytes was quantified by the IFNγ production of activated T cells.

peptide.[41] Howard et al.[42] effectively scavenged PMB cations using phenol as an electron-rich aromatic additive, and when this additive was applied here, the quality of the crude mixture indeed improved. Further optimization of the cleavage conditions was achieved by increasing the concentration of the scavengers (up to 10% of the total volume) and increasing the volume of the cleavage medium (effectively diluting the concentration of reactive cationic species and reactive functional groups). Using this optimized cleavage protocol, all four peptides were successfully deprotected and released from the resin. After RP-HPLC purification, the monovalent *C*-mannose conjugate **39** was obtained in 2.6% yield after 36 coupling steps and the hexavalent *C*-mannose conjugate **40** in 1.3% yield over 41 couplings. The conjugates **41** and **42** were isolated in 2.1% (after 36 steps) and 0.6% (after 41 couplings), respectively (Scheme 3). Unlike the *O*-mannoside conjugates we previously generated, these constructs did not require additional conjugation and purification steps.

https://dx.doi.org/10.1021/acschembio.9b00987
ACS Chem. Biol. XXXX, XXX, XXX−XXX

To compare the activity of the *C*- vs the *O*-mannoside conjugates, *O*-mannoside clusters **24** and **27** were functionalized with an alkyne handle (yielding **43** and **44**) and conjugated through a CuAAC ligation to the TLR7L- gp100 peptide **45** to obtain analogs **46** and **47**.

Mannosylated gp100 Conjugate Efficacy As Vaccination Strategy. We analyzed the influence of the *C*-mannosylated antigens on dendritic cell maturation, cytokine secretion, and antigen presentation to $CD4^+$ and $CD8^+$ T lymphocytes in relation to their *O*-mannosylated peptide counterpart (Figure 2A). Furthermore, the effect of C versus N terminal ligation of the TLR7 ligand was assessed.

Dendritic cell maturation is considered an essential requirement for proper T lymphocyte activation and polarization. As a measure of DC maturation, we quantified expression of the costimulatory molecules CD86 (Figure 2B) and CD83 (see SI, Figure SI.1D) using the six variants of the trivalent conjugates. The nonglycosylated gp100 **48** and the bivalent gp100-TLR7L conjugate **49** were included as controls. After overnight stimulation with the conjugates, we found that all conjugates induced expression of CD86 and CD83. The *C*-mannoside conjugates did not hamper the DC maturation processes and effectively elevated expression levels to the same extent as the *O*-mannosylated conjugates. The position to which the TLR7 agonist was attached does not seem to affect the maturation of the DCs in this assay.

During maturation, DCs produce and secrete a tailored cytokine cocktail for subsequent T lymphocyte skewing. The secreted cytokine profile depends on the triggered TLR, the signaling pathway of which can be modified by DC-SIGN or other CLR engagement.[43] To assess DC activation, we quantified four key cytokines using a sandwich ELISA. IL-6 and IL-12 are primarily characterized as pro-inflammatory cytokines, with functions aiding DC maturation and Th1 stimulation, respectively. Tumor necrosis factor (TNF)-α is required for DC activation and proliferation and reduces IL-10 mediated inhibition during DC development.[44] IL-10 is a cytokine that interferes with DC maturation and inhibits the production of IL-12 and, as such, has been implied to play a role in skewing of naïve T lymphocytes to Treg differentiation.[45] Low levels of autocrine IL-10 prevent spontaneous maturation of DCs.[46] Figure 2C shows that the stand-alone peptide (**48**) and gp100-TLR7L (**49**) minimally induced the production of IL-6, while both the monovalent and hexavalent *O*-mannoside trifunctional conjugates **46** and **47** increased the secretion of this pro-inflammatory cytokine. The monovalent and hexavalent *C*-mannoside conjugates **41** and **42** increased the IL-6 levels to a similar extent as their *O*-mannoside counterparts. However, when moDCs were stimulated with conjugates **39** and **40**, having both the *C*-mannosides and the TLR7L attached to the *N*-terminus of the peptide sequence, cytokine production was abrogated. A similar pattern was observed for the IL-12 production profile: the *O*- and *C*-mannose conjugates having the TLR7 ligand at the C-terminus of the conjugate were most active in stimulating the production of this cytokine, while the gp100 peptide and gp100 peptide-TLR7L conjugate were less active. The conjugates **39** and **40** induced low levels of the IL-12 cytokine. TNF-α expression levels were minimally affected upon stimulation of the DCs with the various conjugates. Also here, the conjugates carrying the TLR7 ligand and the mannosides on the same side of the peptide antigen showed the least activation. Finally, a low level of the anti-inflammatory IL-10 was detected in the ELISA with the nonstimulated DCs, as well as for those treated with peptide **49**. Figure 2C shows that while LPS effectively triggers the production of IL-10, the mannosylated conjugates do not induce the production of this cytokine. Overall the cytokine production profiles of the *O*- and *C*-mannose conjugates appear to be very similar for both the monovalent and hexavalent clusters. In addition, these experiments revealed that the arrangement of the CLR and TLR ligands within the trifunctional conjugates has a great influence on the activity of the conjugates. Possibly, the processing of these conjugates is different from the conjugates bearing the CLR and TLR ligand on either side of the conjugate, due to differential cleavage of the conjugates by proteases.

Finally, we studied the antigen presentation capacity of the DCs upon stimulation with all the trifunctional conjugate variations. During DC maturation, the intrinsic focus of these cells shifts from antigen endocytosis to antigen processing, major histocompatibility complex (MHC) molecule loading, and presentation of the antigens for initiation of the T cell response. Upon recognition of the cross-presented antigen in MHC-I, cytotoxic $CD8^+$ T cells induce programmed cell death of targeted cells. On the other hand, $CD4^+$ T lymphocytes induce and support a cellular and humoral response upon antigen-MHC-II binding. As both T-cell responses are needed for a robust immune response, we studied the antigen (gp100) presenting capacity of the DCs to both $CD8^+$ and $CD4^+$ T cells after stimulation with the trifunctional conjugates.[47] To this end, DCs were stimulated for 30 min with the conjugates, before washing and coculturing with the $CD8^+$ HLA-A2.1 or $CD4^+$ HLA-DR4.1 restricted T cell clone for 24 h. Activation of T cells was measured by quantification of the IFNγ cytokine produced. As shown in Figure 2D, the conjugates carrying a TLR7 ligand are more active than the stand-alone peptide, except for conjugate **40**. The introduction of a CLR ligand also increases the antigen-presenting activity of the conjugates, although the hexavalent *C*-mannoside conjugate appears to hamper antigen presentation with respect to the monovalent conjugate partially. The presence of the TLR7 ligand and the hexavalent mannoside cluster on the same side of the conjugate blocks $CD8^+$ antigen presentation, likely as the result of suboptimal processing. In our previous study, in which we have investigated gp100 conjugates bearing hexavalent clusters comprising di- and trimannosides, we found that the α1,2-dimannoside cluster gp100 conjugates, although being the best DC-SIGN binders, showed less antigen presentation than a gp100-TLR7 conjugate lacking the carbohydrate cluster. Clusters composed of α1,3- and α1,6-linked dimannosides or α1,3-α1,6-linked trimannosides showed slightly enhanced antigen presentation. Taken together, these results show that optimal antigen presentation requires not only DC-SIGN binding but also adequate processing of the incorporated antigens. These results were substantiated by the $CD4^+$ T cell activation assay, as similar gp100 antigen presentation effects were seen (Figure 2E). Monovalent *O*- and *C*-mannosyl conjugates **46** and **41** improved antigen presentation to $CD4^+$ T cells most, and attachment of the TLR7 ligand to the same side as the CLR ligand again nullified activity of the conjugates. Overall, also in these assays, the *O*- and *C*-mannosides perform similarly. The combined results from the assays in Figure 2 show that the most attractive vaccine conjugates require the antigenic peptide to be placed between an N-terminal CLR

https://dx.doi.org/10.1021/acschembio.9b00987
ACS Chem. Biol. XXXX, XXX, XXX−XXX

ligand and a C-terminal TLR-ligand for antigen presentation and secretion cell activation.

CONCLUSION

In conclusion, we have developed a *C*-mannosyl lysine that can be effectively used in solid-phase peptide synthesis (SPPS) campaigns. The stability of the *C*-glycosidic linkage renders the mannoside stable to both acidic reaction conditions employed during SPPS and enzymatic degradation. The protecting groups on the building block were designed to be compatible with standard SPPS protocols to allow the straightforward "in-line" incorporation of the mannosylated residues in oligopeptides. This allows for the generation of mannosylated conjugates without the necessity of a postassembly conjugation step requiring orthogonal click strategies. Not only does this streamline the synthesis of these conjugates, it also ensures that bio-orthogonal handles, such as azides and alkynes, can be incorporated into these multifunctional antigen conjugates to allow these for the incorporation of additional functionalities, such as other immune stimulating agents or fluorophores. We have applied the mannosylated lysine in the assembly of a set of synthetic long peptide antigens to equip these with either one or six mannosides to target the antigens to mannose-binding C-type lectins on professional antigen-presenting cells to improve the antigenicity of the peptides. The conjugates were further armed with a synthetic TLR7 ligand to further boost the response against the antigens. In comparing the *C*- vs the *O*-mannosylated conjugates for DC-SIGN mediated uptake, DC maturation, and stimulation as well as $CD4^+$ and $CD8^+$ antigen presentation, the stabilized mannosides performed virtually identically to their natural analogs. The conjugates bearing the mannosides and a TLR7 ligand were shown to bind DC-SIGN and activate DCs, as indicated by pro-inflammatory cytokine release, upregulation of cell surface maturation markers, and increased antigen presentation to both $CD4^+$ and $CD8^+$ lymphocytes. Notably, the relative position of the CLR and TLR ligands in the peptide antigen conjugates played an important role in shaping the activity of the conjugates. The conjugates bearing the mannose cluster and the TLR7 ligand on the same side of the conjugates proved to be poor immune-stimulating agents, incapable of elucidating an effective pro-inflammatory response and showing poor antigen presentation. These differences are likely due to differences in the processing of the conjugates. As DC vaccination therapies hold great promise as an immunotherapeutic approach to fight cancer, the development of more effective, tailor-made cancer vaccine conjugates, of which the action is well understood and can be controlled, is of great importance. The conjugates described here can be further equipped with biorthogonal visualization handles to allow tracking of the conjugates during uptake and processing. Because the *C*-mannosyl lysine building block can be incorporated in an "in-line" manner and does not rely on a postassembly conjugation step, often used biorthogonal coupling partners, such as azides and alkynes, remain at one's disposal for inclusion in the conjugates.

METHODS

Synthesis. The synthesis of *C*-mannosyl **1** and all clusters and conjugates is described in the Supporting Information.

Cell Isolation and Culture. Buffy coats of healthy donors were obtained from Sanquin Amsterdam (reference: S03.0023-XT). Monocytes were isolated using a Ficoll (STEMCELL Technologies) and sequential Percoll (Sigma) gradient centrifugation. The monocytes were differentiated to monocyte-derived dendritic cells (moDCs) in RPMI 1640 (Invitrogen), supplemented with 10% FCS (Biowittaker), 1.000 U/mL penicillin (Lonza), 1 U/mL streptomycin (Lonza), 262.5 U/mL IL-4 (Biosource), and 112.5 U/mL GM-CSF (Biosource), for 5 days. Flow cytometric monitoring of DC-SIGN (AZN-D1-Alexa488, in house[48]), CD83, and CD86 (both PE-conjugated, Becton Dickinson) expression was conducted for every donor.

Binding of the Mannose Clusters to moDCs. Day 5 moDCs (approximately 10^5 per condition) were washed and resuspended in ice-cold RPMI medium (Invitrogen). The entire experiment was conducted at 4 °C with precooled reagents. DC-SIGN and mannose receptor were blocked with 20 μg/mL AZN-D1 (in house[48]) and purified mouse antihuman CD206 antibody (Clone 19.2, BD Bioscience), respectively, for 45 min. The biotinylated mannoside clusters (10 μM) or $Lewis^Y$-conjugated polyacrylamide (1 μg/mL) as positive control was allowed to bind for 30 min. The moDCs were washed with PBS and stained with an Alexa647-labeled streptavidin (Invitrogen) in PBS supplemented with 0.5% BSA and 0.02% NaN_3 (PBA) for 30 min. The moDCs were subsequently washed and fixed in PBS with 0.5% PFA, before the fluorescence was measured by flow cytometry (CyAn ADP with Summit Software) and analyzed using FlowJo v10.

Internalization of the Mannoside Clusters. Day 5 moDCs (approximately 10^5 per condition) were washed and resuspended in ice-cold HBSS medium (Thermo Fischer). The biotinylated mannoside clusters (20 μM) were added in ice-cold medium to the moDCs for 1 h and washed away with ice-cold medium. Prewarmed HBSS (37 °C) was added to the cells and was incubated at 37 °C in a shaking heating block (800 rpm). Samples of the cells were taken at the indicated time points (t = 0, 5, 10, 15, 30, 60 min) and immediately put on ice. The moDCs were washed with ice-cold PBS supplemented with 0.5% BSA and 0.02% NaN_3 (PBA) and stained with Alexa647-labeled streptavidin (InvitrogenTM) for 30 min at 4 °C. The fluorescence was measured by flow cytometry (CyAn ADP with Summit Software) and analyzed using FlowJo v10.

Endosomal Routing of the Mannoside Clusters. Day 5 moDCs (approximately 10^5 per condition) were washed and resuspended in prewarmed (37 °C) HBSS medium (Thermo Fischer). The biotinylated mannoside clusters (20 μM) were complexed with pHrodo (2:1 ratio) for 15 min at RT. The precomplexed pHrodo-labeled ligands were added to the cells and were incubated at 37 °C in a shaking heating block (800 rpm). Samples of the cells were taken at the indicated time points (t = 0, 5, 10, 15, 30, 60, 120 min) and immediately put on ice. The moDCs were washed with ice-cold PBS supplemented with 0.5% BSA and 0.02% NaN_3 (PBA). The fluorescence was measured by flow cytometry (BD LSRFortessa X-20 with FACSDiva Software) and analyzed using FlowJo v10.

moDC Cytokine Secretion upon Stimulation with the Mannoside Clusters. Day 5 moDCs (approximately 50×10^5 per condition) were stimulated for 24 h with the trifunctional conjugates. Cytokines IL-6, IL-10, IL-12p40, and TNFα in the supernatant were measured by sandwich ELISA according to manufacturer's protocol (Biosource). The capture antibody was coated in NUNC MaxiSorp plates (Nunc, Roskilde, Denmark) overnight at 4 °C in PBA-0.05% BSA. The plates were blocked for 30 min at 37 °C, using PBS supplemented with 1% BSA. Samples were added for 2 h at RT to allow binding and subsequently washed, and cytokine levels were detected using a peroxidase-conjugated cytokine-specific detection antibody. After extensive washing, the binding was visualized with 3,3′,5,5′-tetramethylbenzidine (Sigma-Aldrich) and measured by spectrophotometry at 450 nm on the iMark Microplate Absorbance Reader (Bio-RAD).

$CD4^+$ and $CD8^+$ Antigen Presentation. Day 5 moDCs of HLA-A2 and HLA-DR4 double positive donors (approximately 40×10^3 per condition) were incubated with the different trifunctional conjugates (20 μM) for 30 min at 37 °C. A short gp100 peptide ($gp100_{280-288}$) and a long gp100 peptide ($gp100_{280-288,40-59}$) were

https://dx.doi.org/10.1021/acschembio.9b00987
ACS Chem. Biol. XXXX, XXX, XXX−XXX

used as controls. The moDCs were washed and separated into two plates (30×10^3 for $CD8^+$ and 10×10^3 for $CD4^+$ T lymphocyte coculture). Either a $CD8^+$ HLA-A2.1 restricted T cell clone transduced with the TCR specific for the $gp100_{280-288}$ peptide[49] (approximately 10^5 cells per condition, E/T ratio 1:3) or a $CD4^+$ HLA-DR4.1 restricted T cell clone transduced with the TCR specific for the $gp100_{44-59}$ peptide (approximately 10^5 cells per condition, E/T ratio 1:10) was added for overnight coculture. The interferon γ cytokine secretion was measured by sandwich ELISA, according to the manufacturer's protocol (Biosource), and measured by spectrophotometric analysis at 450 nm on the iMark Microplate Absorbance Reader (Bio-RAD).

Statistics. Unless otherwise stated, data are presented as the mean ± SD of at least three independent experiments or healthy donors. Statistical analyses were performed in GraphPad Prism v7.04. Statistical significance was set at $P < 0.05$, and it was evaluated by the Mann–Whitney U test.

■ ASSOCIATED CONTENT

Supporting Information

The Supporting Information is available free of charge at https://pubs.acs.org/doi/10.1021/acschembio.9b00987.

All other synthetic procedures, supporting figures, NMR spectra, and HPLC spectra (PDF)

■ AUTHOR INFORMATION

Corresponding Authors

Yvette van Kooyk − *Amsterdam UMC-Location Vrije Universiteit Amsterdam, Deptartment of Molecular Cell Biology and Immunology, Cancer Center Amsterdam, Amsterdam Infection and Immunity Institute, Amsterdam, Netherlands*; Email: Y.vanKooyk@amsterdamumc.nl

Jeroen D. C. Codée − *Department of Bio-organic Synthesis, Faculty of Science, Leiden Institute of Chemistry, Leiden University, Leiden, The Netherlands*; orcid.org/0000-0003-3531-2138; Email: JCodee@chem.leidenuniv.nl

Authors

Tim P. Hogervorst − *Department of Bio-organic Synthesis, Faculty of Science, Leiden Institute of Chemistry, Leiden University, Leiden, The Netherlands*; orcid.org/0000-0002-4686-6251

R. J. Eveline Li − *Amsterdam UMC-Location Vrije Universiteit Amsterdam, Deptartment of Molecular Cell Biology and Immunology, Cancer Center Amsterdam, Amsterdam Infection and Immunity Institute, Amsterdam, Netherlands*

Laura Marino − *Department of Bio-organic Synthesis, Faculty of Science, Leiden Institute of Chemistry, Leiden University, Leiden, The Netherlands*

Sven C. M. Bruijns − *Amsterdam UMC-Location Vrije Universiteit Amsterdam, Deptartment of Molecular Cell Biology and Immunology, Cancer Center Amsterdam, Amsterdam Infection and Immunity Institute, Amsterdam, Netherlands*

Nico J. Meeuwenoord − *Department of Bio-organic Synthesis, Faculty of Science, Leiden Institute of Chemistry, Leiden University, Leiden, The Netherlands*

Dmitri V. Filippov − *Department of Bio-organic Synthesis, Faculty of Science, Leiden Institute of Chemistry, Leiden University, Leiden, The Netherlands*; orcid.org/0000-0002-6978-7425

Herman S. Overkleeft − *Department of Bio-organic Synthesis, Faculty of Science, Leiden Institute of Chemistry, Leiden University, Leiden, The Netherlands*; orcid.org/0000-0001-6976-7005

Gijsbert A. van der Marel − *Department of Bio-organic Synthesis, Faculty of Science, Leiden Institute of Chemistry, Leiden University, Leiden, The Netherlands*

Sandra J. van Vliet − *Amsterdam UMC-Location Vrije Universiteit Amsterdam, Deptartment of Molecular Cell Biology and Immunology, Cancer Center Amsterdam, Amsterdam Infection and Immunity Institute, Amsterdam, Netherlands*

Complete contact information is available at: https://pubs.acs.org/10.1021/acschembio.9b00987

Author Contributions

[§]These authors have contributed equally to this work

Author Contributions

T.P.H. and R.J.E.L. equally contributed to the work and both wrote the manuscript. The compounds were synthesized by T.P.H., assisted by L.M., under the supervision of H.S.O., D.V.F., G.A.v.d.M., and J.D.C.C. N.J.M. aided in the peptide synthesis and purification of certain constructs. R.J.E.L. executed the binding, internalization, endosomal tracking, maturation, and cytokine secretion experiments, and was assisted by S.C.M.B. in the antigen presentation assay, supervised by S.J.v.V. and Y.v.K.

Funding

This work was funded by the NWO gravitation program 2013 granted to the Institute for Chemical Immunology (ICI-024.002.009).

Notes

The authors declare no competing financial interest.

■ REFERENCES

(1) Khair, D. O., Bax, H. J., Mele, S., Crescioli, S., Pellizzari, G., Khiabany, A., Nakamura, M., Harris, R. J., French, E., Hoffmann, R. M., Williams, I. P., Cheung, A., Thair, B., Beales, C. T., Touizer, E., Signell, A. W., Tasnova, N. L., Spicer, J. F., Josephs, D. H., Geh, J. L., MacKenzie Ross, A., Healy, C., Papa, S., Lacy, K. E., and Karagiannis, S. N. (2019) Combining Immune Checkpoint Inhibitors: Established and Emerging Targets and Strategies to Improve Outcomes in Melanoma. *Front. Immunol. 10*, 453.

(2) Boyiadzis, M. M., Dhodapkar, M. V., Brentjens, R. J., Kochenderfer, J. N., Neelapu, S. S., Maus, M. V., Porter, D. L., Maloney, D. G., Grupp, S. A., Mackall, C. L., June, C. H., and Bishop, M. R. (2018) Chimeric Antigen Receptor (CAR) T Therapies for the Treatment of Hematologic Malignancies: Clinical Perspective and Significance. *J. Immunother. Cancer 6*, 137.

(3) Rohaan, M. W., van den Berg, J. H., Kvistborg, P., and Haanen, J. B. A. G. (2018) Adoptive Transfer of Tumor-Infiltrating Lymphocytes in Melanoma: A Viable Treatment Option. *J. Immunother. Cancer 6*, 102.

(4) Huber, A., Dammeijer, F., Aerts, J. G. J. V, and Vroman, H. (2018) Current State of Dendritic Cell-Based Immunotherapy: Opportunities for in Vitro Antigen Loading of Different DC Subsets? *Front. Immunol. 9*, 2804.

(5) Schreibelt, G., Bol, K. F., Westdorp, H., Wimmers, F., Aarntzen, E. H. J. G., Duiveman-de Boer, T., van de Rakt, M. W. M. M., Scharenborg, N. M., de Boer, A. J., Pots, J. M., Olde Nordkamp, M. A. M., van Oorschot, T. G. M., Tel, J., Winkels, G., Petry, K., Blokx, W. A. M., van Rossum, M. M., Welzen, M. E. B., Mus, R. D. M., Croockewit, S. A. J., Koornstra, R. H. T., Jacobs, J. F. M., Kelderman, S., Blank, C. U., Gerritsen, W. R., Punt, C. J. A., Figdor, C. G., and de Vries, I. J. M. (2016) Effective Clinical Responses in Metastatic Melanoma Patients after Vaccination with Primary Myeloid Dendritic Cells. *Clin. Cancer Res. 22*, 2155–2166.

(6) Anguille, S., Smits, E. L., Lion, E., van Tendeloo, V. F., and Berneman, Z. N. (2014) Clinical Use of Dendritic Cells for Cancer Therapy. *Lancet Oncol. 15*, e257–e267.

(7) Ho, N. I., Huis in 't Veld, L. G. M., Raaijmakers, T. K., and Adema, G. J. (2018) Adjuvants Enhancing Cross-Presentation by Dendritic Cells: The Key to More Effective Vaccines? *Front. Immunol. 9*, 2874.
(8) Blander, J. M., and Medzhitov, R. (2006) Toll-Dependent Selection of Microbial Antigens for Presentation by Dendritic Cells. *Nature 440*, 808−812.
(9) Cho, H. J., Takabayashi, K., Cheng, P.-M., Nguyen, M.-D., Corr, M., Tuck, S., and Raz, E. (2000) Immunostimulatory DNA-Based Vaccines Induce Cytotoxic Lymphocyte Activity by a T-Helper Cell-Independent Mechanism. *Nat. Biotechnol. 18*, 509−514.
(10) Deres, K., Schild, H., Wiesmüller, K.-H., Jung, G., and Rammensee, H.-G. (1989) In Vivo Priming of Virus-Specific Cytotoxic T Lymphocytes with Synthetic Lipopeptide Vaccine. *Nature 342*, 561−564.
(11) Fujita, Y., and Taguchi, H. (2012) Overview and Outlook of Toll-like Receptor Ligand−Antigen Conjugate Vaccines. *Ther. Delivery 3*, 749−760.
(12) Willems, M. M. J. H. P., Zom, G. G., Khan, S., Meeuwenoord, N., Melief, C. J. M., van der Stelt, M., Overkleeft, H. S., Codee, J. D. C., van der Marel, G. A., Ossendorp, F., and Filippov, D. V. (2014) N -Tetradecylcarbamyl Lipopeptides as Novel Agonists for Toll-like Receptor 2. *J. Med. Chem. 57*, 6873−6878.
(13) Ignacio, B. J., Albin, T. J., Esser-Kahn, A. P., and Verdoes, M. (2018) Toll-like Receptor Agonist Conjugation: A Chemical Perspective. *Bioconjugate Chem. 29*, 587−603.
(14) Khan, S., Bijker, M. S., Weterings, J. J., Tanke, H. J., Adema, G. J., van Hall, T., Drijfhout, J. W., Melief, C. J. M., Overkleeft, H. S., van der Marel, G. A., Filippov, D. V., van der Burg, S. H., and Ossendorp, F. (2007) Distinct Uptake Mechanisms but Similar Intracellular Processing of Two Different Toll-like Receptor Ligand-Peptide Conjugates in Dendritic Cells. *J. Biol. Chem. 282*, 21145−21159.
(15) Gringhuis, S. I., den Dunnen, J., Litjens, M., van der Vlist, M., and Geijtenbeek, T. B. H. (2009) Carbohydrate-Specific Signaling through the DC-SIGN Signalosome Tailors Immunity to Mycobacterium Tuberculosis, HIV-1 and Helicobacter Pylori. *Nat. Immunol. 10*, 1081−1088.
(16) Bertolotti, B., Sutkeviciute, I., Ambrosini, M., Ribeiro-Viana, R., Rojo, J., Fieschi, F., Dvořáková, H., Kašáková, M., Parkan, K., Hlaváčková, M., Nováková, K., and Moravcová, J. (2017) Polyvalent C-Glycomimetics Based on l -Fucose or d -Mannose as Potent DC-SIGN Antagonists. *Org. Biomol. Chem. 15*, 3995−4004.
(17) White, K. L., Rades, T., Furneaux, R. H., Tyler, P. C., and Hook, S. (2006) Mannosylated Liposomes as Antigen Delivery Vehicles for Targeting to Dendritic Cells. *J. Pharm. Pharmacol. 58*, 729−737.
(18) Sangabathuni, S., Vasudeva Murthy, R., Chaudhary, P. M., Surve, M., Banerjee, A., and Kikkeri, R. (2016) Glyco-Gold Nanoparticle Shapes Enhance Carbohydrate-Protein Interactions in Mammalian Cells. *Nanoscale 8*, 12729−12735.
(19) Ahlén, G., Strindelius, L., Johansson, T., Nilsson, A., Chatzissavidou, N., Sjöblom, M., Rova, U., and Holgersson, J. (2012) Mannosylated Mucin-Type Immunoglobulin Fusion Proteins Enhance Antigen-Specific Antibody and T Lymphocyte Responses. *PLoS One 7*, No. e46959.
(20) Wilson, D. S., Hirosue, S., Raczy, M. M., Bonilla-Ramirez, L., Jeanbart, L., Wang, R., Kwissa, M., Franetich, J.-F., Broggi, M. A. S., Diaceri, G., Quaglia-Thermes, X., Mazier, D., Swartz, M. A., and Hubbell, J. A. (2019) Antigens Reversibly Conjugated to a Polymeric Glyco-Adjuvant Induce Protective Humoral and Cellular Immunity. *Nat. Mater. 18*, 175−185.
(21) Li, R.-J. E., Hogervorst, T. P., Achilli, S., Bruijns, S. C., Arnoldus, T., Vivès, C., Wong, C. C., Thépaut, M., Meeuwenoord, N. J., van den Elst, H., Overkleeft, H. S., van der Marel, G. A., Filippov, D. V., van Vliet, S. J., Fieschi, F., Codée, J. D. C. C., and van Kooyk, Y. (2019) Systematic Dual Targeting of Dendritic Cell C-Type Lectin Receptor DC-SIGN and TLR7 Using a Trifunctional Mannosylated Antigen. *Front. Chem. 7*, DOI: 10.3389/fchem.2019.00650.
(22) Tamburrini, A., Colombo, C., and Bernardi, A. (2020) Design and Synthesis of Glycomimetics: Recent Advances. *Med. Res. Rev. 40*, 495.
(23) Zou, W. (2005) C-Glycosides and Aza-C-Glycosides as Potential Glycosidase and Glycosyltransferase Inhibitors. *Curr. Top. Med. Chem. 5*, 1363−1391.
(24) Girard, C., Miramon, M., de Solminihac, T., and Herscovici, J. (2002) Synthesis of 3-C-(6-O-Acetyl-2,3,4-Tri-O-Benzyl-α-d-Manno-pyranosyl)-1-Propene: A Caveat. *Carbohydr. Res. 337*, 1769−1774.
(25) Jarikote, D. V., O'Reilly, C., and Murphy, P. V. (2010) Ultrasound-Assisted Synthesis of C-Glycosides. *Tetrahedron Lett. 51*, 6776−6778.
(26) Touaibia, M., Krammer, E.-M., Shiao, T., Yamakawa, N., Wang, Q., Glinschert, A., Papadopoulos, A., Mousavifar, L., Maes, E., Oscarson, S., Vergoten, G., Lensink, M., Roy, R., and Bouckaert, J. (2017) Sites for Dynamic Protein-Carbohydrate Interactions of O- and C-Linked Mannosides on the E. Coli FimH Adhesin. *Molecules 22*, 1101.
(27) Sharma, P. K., Kumar, S., Kumar, P., and Nielsen, P. (2007) Selective Reduction of Mono- and Disubstituted Olefins by NaBH4 and Catalytic RuCl3. *Tetrahedron Lett. 48*, 8704−8708.
(28) Newlander, K. A., Callahan, J. F., Moore, M. L., Tomaszek, T. A., and Huffman, W. F. (1993) A Novel Constrained Reduced-Amide Inhibitor of HIV-1 Protease Derived from the Sequential Incorporation of.Gamma.-Turn Mimetics into a Model Substrate. *J. Med. Chem. 36*, 2321−2331.
(29) Boger, D. L., Yohannes, D., Zhou, J., and Patane, M. A. (1993) Total Synthesis of Cycloisodityrosine, RA-VII, Deoxybouvardin, and N29-Desmethyl-RA-VII: Identification of the Pharmacophore and Reversal of the Subunit Functional Roles. *J. Am. Chem. Soc. 115*, 3420−3430.
(30) Jencks, W. P., and Gilchrist, M. (1968) Nonlinear Structure-Reactivity Correlations. The Reactivity of Nucleophilic Reagents toward Esters. *J. Am. Chem. Soc. 90*, 2622−2637.
(31) Raiber, E.-A., Tulone, C., Zhang, Y., Martinez-Pomares, L., Steed, E., Sponaas, A. M., Langhorne, J., Noursadeghi, M., Chain, B. M., and Tabor, A. B. (2010) Targeted Delivery of Antigen Processing Inhibitors to Antigen Presenting Cells via Mannose Receptors. *ACS Chem. Biol. 5*, 461−476.
(32) pHrodo Indicators for pH Determination - NL. https://www.thermofisher.com/nl/en/home/brands/molecular-probes/key-molecular-probes-products/phrodo-indicators.html (accessed Sep 3, 2019).
(33) Hotta, C., Fujimaki, H., Yoshinari, M., Nakazawa, M., and Minami, M. (2006) The Delivery of an Antigen from the Endocytic Compartment into the Cytosol for Cross-Presentation Is Restricted to Early Immature Dendritic Cells. *Immunology 117*, 97−107.
(34) Zhang, S., Li, J., Lykotrafitis, G., Bao, G., and Suresh, S. (2009) Size-Dependent Endocytosis of Nanoparticles. *Adv. Mater. 21*, 419−424.
(35) Vennepureddy, A., Thumallapally, N., Nehru, V. M., Atallah, J.-P., and Terjanian, T. (2016) Novel Drugs and Combination Therapies for the Treatment of Metastatic Melanoma. *J. Clin. Med. Res. 8*, 63−75.
(36) Chan, M., Hayashi, T., Kuy, C. S., Gray, C. S., Wu, C. C. N., Corr, M., Wrasidlo, W., Cottam, H. B., and Carson, D. A. (2009) Synthesis and Immunological Characterization of Toll-Like Receptor 7 Agonistic Conjugates. *Bioconjugate Chem. 20*, 1194−1200.
(37) Wlodawer, A., Miller, M., Jaskolski, M., Sathyanarayana, B., Baldwin, E., Weber, I., Selk, L., Clawson, L., Schneider, J., and Kent, S. (1989) Conserved Folding in Retroviral Proteases: Crystal Structure of a Synthetic HIV-1 Protease. *Science (Washington, DC, U. S.) 245*, 616−621.
(38) Gential, G. P. P., Hogervorst, T. P., Tondini, E., van de Graaff, M. J., Overkleeft, H. S., Codée, J. D. C., van der Marel, G. A., Ossendorp, F., and Filippov, D. V. (2019) Peptides Conjugated to 2-Alkoxy-8-Oxo-Adenine as Potential Synthetic Vaccines Triggering TLR7. *Bioorg. Med. Chem. Lett. 29*, 1340−1344.

https://dx.doi.org/10.1021/acschembio.9b00987
ACS Chem. Biol. XXXX, XXX, XXX−XXX

(39) Chan, M., Hayashi, T., Kuy, C. S., Gray, C. S., Wu, C. C. N., Corr, M., Wrasidlo, W., Cottam, H. B., and Carson, D. A. (2009) Synthesis and Immunological Characterization of Toll-Like Receptor 7 Agonistic Conjugates. *Bioconjugate Chem. 20*, 1194−1200.
(40) Matysiak, S., Böldicke, T., Tegge, W., and Frank, R. (1998) Evaluation of Monomethoxytrityl and Dimethoxytrityl as Orthogonal Amino Protecting Groups in Fmoc Solid Phase Peptide Synthesis. *Tetrahedron Lett. 39*, 1733−1734.
(41) Volbeda, A. G., Kistemaker, H. A. V., Overkleeft, H. S., van der Marel, G. A., Filippov, D. V., and Codée, J. D. C. (2015) Chemoselective Cleavage of *p* -Methoxybenzyl and 2-Naphthylmethyl Ethers Using a Catalytic Amount of HCl in Hexafluoro-2-Propanol. *J. Org. Chem. 80*, 8796−8806.
(42) Howard, K. T., and Chisholm, J. D. (2016) Preparation and Applications of 4-Methoxybenzyl Esters in Organic Synthesis. *Org. Prep. Proced. Int. 48*, 1−36.
(43) Geijtenbeek, T. B. H., and Gringhuis, S. I. (2016) C-Type Lectin Receptors in the Control of T Helper Cell Differentiation. *Nat. Rev. Immunol. 16*, 433−448.
(44) Brossart, P., Zobywalski, A., Grünebach, F., Behnke, L., Stuhler, G., Reichardt, V. L., Kanz, L., and Brugger, W. (2000) Tumor Necrosis Factor Alpha and CD40 Ligand Antagonize the Inhibitory Effects of Interleukin 10 on T-Cell Stimulatory Capacity of Dendritic Cells. *Cancer Res. 60*, 4485−4492.
(45) de Smedt, T., van Mechelen, M., De Becker, G., Urbain, J., Leo, O., and Moser, M. (1997) Effect of Interleukin-10 on Dendritic Cell Maturation and Function. *Eur. J. Immunol. 27*, 1229−1235.
(46) Corinti, S., Albanesi, C., la Sala, A., Pastore, S., and Girolomoni, G. (2001) Regulatory Activity of Autocrine IL-10 on Dendritic Cell Functions. *J. Immunol. 166*, 4312−4318.
(47) Wieczorek, M., Abualrous, E. T., Sticht, J., Álvaro-Benito, M., Stolzenberg, S., Noé, F., and Freund, C. (2017) Major Histocompatibility Complex (MHC) Class I and MHC Class II Proteins: Conformational Plasticity in Antigen Presentation. *Front. Immunol. 8*, 292.
(48) Engering, A., Geijtenbeek, T. B. H., van Vliet, S. J., Wijers, M., van Liempt, E., Demaurex, N., Lanzavecchia, A., Fransen, J., Figdor, C. G., Piguet, V., and van Kooyk, Y. (2002) The Dendritic Cell-Specific Adhesion Receptor DC-SIGN Internalizes Antigen for Presentation to T Cells. *J. Immunol. 168*, 2118−2126.
(49) Schaft, N., Willemsen, R. A., de Vries, J., Lankiewicz, B., Essers, B. W. L., Gratama, J.-W., Figdor, C. G., Bolhuis, R. L. H., Debets, R., and Adema, G. J. (2003) Peptide Fine Specificity of Anti-Glycoprotein 100 CTL Is Preserved Following Transfer of Engineered TCR Genes Into Primary Human T Lymphocytes. *J. Immunol. 170*, 2186−2194.

https://dx.doi.org/10.1021/acschembio.9b00987
ACS Chem. Biol. XXXX, XXX, XXX−XXX